*Recent Patents on Drug Delivery & Formulation* 2019, *13*, 228-240

RESEARCH ARTICLE

# Application of Optimization Technique to Develop Nano-Based Carrier of *Nigella sativa* Essential Oil: Characterization and Assessment

Aya M. Dawaba[1,*] and Hamdy M. Dawaba[2]

[1]*Department of Pharmaceutics, Faculty of Pharmacy (Girls), Al-Azhar University, Cairo, Egypt;* [2]*Department of Pharmaceutics, Faculty of Pharmacy (Boys), Al-Azhar University, Cairo, Egypt*

**Abstract:** ***Background*:** Chitosan, a naturally occurring polymer, has interesting applications in the field of drug delivery due to its plentiful advantages as biodegradability, biocompatibility and nontoxic nature. *Nigella sativa* essential oil is unstable, volatile, and insoluble in water and these problems confine its usage in developing new medicines.

***Objective*:** This study focuses on developing a chitosan-based nanocarrier for the encapsulation of *Nigella Sativa* essential oil. By using Quality by design outline, the quality target product outline, critical quality attributes and critical material attributes were defined by knowledge and risk-based procedures.

***Methods*:** According to defined critical material attributes, Optimization software (Statgraphics XVII) was used to study the effect of the processing parameters. The processing parameters identified and fixed first with a "One factor at a time" approach. Various physicochemical characterization techniques were performed.

***Results*:** As a result, the ratio of chitosan to benzoic acid (2:1) along with the stirring rate (4000 rpm) produced minimum-sized particles (341 nm) with good stability. The anti-bacterial activity study using *Staph. Aureus strain* proved that the optimized nanoparticles were more efficacious than the pure oil based on the diameter of inhibition zone obtained (diameter =5.5 cm for optimized formula *vs* diameter = 3.6 cm for pure oil). Furthermore, MTT (methyl thiazolyl-diphenyl-tetrazolium bromide) assay was performed to compare the *in vitro* cytotoxicity using two different cell lines (*i.e*. HCT 116 for colorectal carcinoma and PC3 for prostatic cancer). It was found that in both cell lines, the optimized nanoparticles had noteworthy antiproliferative properties illustrated by determining the concentration at which 50% of growth is inhibited (IC50). The optimized nanoparticles showed lower IC50 (17.95 ±0.82 and 4.02 ±0.12µg/ml) than the bare oil IC50 (43.56 ±1.95 and 29.72 ±1.41µg/ml).

ARTICLE HISTORY

Received: February 24, 2019
Revised: April 27, 2019
Accepted: May 06, 2019

*DOI:*
*10.2174/1872211313666190516095309*

**Keywords:** *Nigella sativa*, chitosan nanoparticles, optimization, one factor at a time, benzoic acid, biodegradability.

## 1. INTRODUCTION

Application of nanotechnology in drug-delivery gives a chance to deliver drugs for a delayed time with natural affinity [1]. Examples of nanocarriers widely employed in the field of drug delivery are dendrimers, micelles, liposomes, and nanoemulsions. These delivery systems enhance the solubility of hydrophobic compounds as well as drugs' biodistribution and bioavailability resulting in reducing the frequency of doses, improving drug targeting, and limiting toxicity [2].

Among the numerous nanocarriers, Chitosan (CS) has gained more consideration because of its biocompatibility, biodegradability, mucoadhesiveness, and longer *in vivo* course time [2-4].

Inside the current competitive and entirely directed condition, the utilization of methodical philosophies is considered significant to enhance performance, limit error and expelling waste, for all sort of industries, just as Pharmaceutical industry. As such, Six Sigma is a standout amongst the most acknowledged arrangements of instruments for process enhancement, which intervene as Quality by Design (QbD) to the pharmaceutical business [5].

Execution of QbD begins with the import of Quality Target Product Profile (QTPP), Critical Quality Attributes (CQAs), Critical Process Parameters (CPPs) and Critical Material Attributes (CMAs) and associates among them, by utilizing efficient hazard-based methodologies.

In science and hazard-based methodology of QbD, the proof of mathematical models is extremely important. In QbD system, scientific models might be first standards, exact, or hybrid models. Among various approaches that generate an observational mathematical model and design space, Design of Experiment (DoE) stands out as the most produc-

*Address correspondence to this author at Department of Pharmaceutics, Faculty of Pharmacy (Girls), Al-Azhar University, Cairo 11651, Egypt; Tel: +201092249996; E-mails: aya.dawaba@yahoo.com; ayadawaba@azhar.edu.eg

2212-4039/19 $58.00+.00 

tive approach. The resultant models of DoE can be utilized for screening or optimization. The expectations from the model, the number and sort of the factors are the basic corners that DoE determination relies on. In QbD structure, choice of the DoE elements can rely upon hazard appraisal or earlier information.

*Nigella sativa L*. is a well-known medicinal food plant with a long history of ethnomedicinal antimicrobial uses [6-8]. Its active ingredients are mainly concentrated in the essential oil of the seed [9]. The plant has been widely used as an analgesic, anti-inflammatory, anticancer, antimicrobial, antioxidant and gastro-protective agent [10]. It has been demonstrated that the therapeutic properties of *N. sativa* are due to the presence of thymoquinone, a major biologically active constituent of the essential oil [9], along with other high-value components such as linoleic acid, nigellone (dithymoquinone), nigilline, melanthin, and trans-anethole [11]. For the latter 2~3 eras, inquiry of the anticancer action of *Nigella Sativa* oil is a relatively recent concern [12-14].

In spite of *Nigella Sativa* Oil (NSO) numerous profits, it has poor physical properties for instance hydrophobicity, unstable and volatile. Hence, the present work was intended to formulate chitosan-based nanoparticles containing NSO utilizing QbD approach to recognize the effects of CMAs on the CQAs of formulation and to create a design to optimize the formulation responses and screening its antimicrobial and anticancer activity.

The main purposes for developing formulations containing Essential Oils (EOs) are to shield the EO from evaporation and degradation, and to achieve a controlled release. Since the EOs exist in a liquid form at room temperature. Subsequently, the simplest form of encapsulation is to emulsify or disperse them in an aqueous solution of the carrier material.

Since CS is non-poisonous, natural, and biocompatible compound, it will pose no danger to live cells. Connecting CS's amino groups to adjacent groups like fatty acids as BA and Ci, produces derivatives which incline to dual bonds, and this feature makes it feasible for them to form nanomicelles in water capable of encapsulating fats and oils *e.g*. herbal essential oils.

## 2. MATERIALS AND METHODS

### 2.1. Materials

Chitosan (CS; *M*w = 100,000– 300,000 Da) with degree of deacetylation >90% (Ward Hill, MA 01835, USA). *N. sativa* oil (NSO; purity 98%) was purchased from Imtnan® company, Cairo, Egypt. Benzoic Acid (BA), Cinnamic acid (Ci) were purchased from Al Nasr pharmaceutical company, Cairo, Egypt. Ethylene Dichloride (EDC) and sodium hydroxide (NaOH), Sodium Lauryl Sulfate (SLS) were purchased from El Gomheria company, Cairo, Egypt. 3-(4,5-dimethylthiazol-2-yl)-2,5-diphenyl tetrazolium bromide (MTT) was purchased from Sigma Aldrich, St. Louis, MO, USA. Human colorectal cancer cells (HC 116; ATTC ® - CCL-247 ™) and human prostate cancer cell line (PC3; ATCC ® CRL- 1435 ™) were obtained from American Type Culture Collection (ATCC, Manassas, VA, USA). Poloxamer 188, Tween 80, glacial acetic acid and methanol AR were a gift sample from Pharco company, Alex., Egypt. Any other reagent was of analytical grade and used without further purification.

### 2.2. Preparation of Chitosan Nanoparticles (CS-NPs)

Chitosan-nanoparticles were fabricated by ionic gelation technique with gentle modification [15-17]. Briefly, 1% acetic acid used to dissolve CS to obtain a final concentration of 1, 2, and 3% by magnetic stirrer (L32; Bibby, Staffordshire, UK) overnight, followed by filtration (0.45 µm Millipore filter). Poloxamer 188 (1%, w/v) and tween 60 were added as stabilizers to CS solution and sonication for 20 min using bath-type sonicator (Model SS101H 230, Sonix IV, CA, USA) was performed followed their addition. BA or Ci solution in EDC was added to CS solution dropwise over 20 min with a syringe under stirring to yield different ratios of CS:BA or Ci (2:1, 1:1, and 1:2). The pH of CS solution was adjusted to 4.8 using NaOH solution (2N).

*N. sativa* loaded CS-NPs were prepared using the aforementioned methodology and ratio. A fixed volume of NSO (2ml) was added to CS solution and sonicated for 5 min before the addition of BA-EDC solution. The prepared dispersions were allowed to stabilize by magnetic stirring for 30 min. CS-NPs were collected by centrifugation at 15000 rpm for 30 min at 4°C (Cooling bench centrifuge, Sigma 3-16K, Germany). The supernatant was removed by aspiration with a syringe needle and used to determine Encapsulation Efficiency (EE). The precipitate was re-dispersed in 5ml deionized water by sonication (bath sonicator, Model SS101H 230, Sonix IV, CA, USA) for 10 min [18].

### 2.3. Determination of Encapsulation Efficacy (EE)

The supernatant was removed by aspiration with a syringe needle and passed into separating funnel and left for 3 days for complete equilibration to estimate the amount of free oil (not encapsulated). The amount of free oil was determined by a validated spectrophotometric method established by Snehalatha *et al*. [19] where a calibration curve was constructed using a standard stock solution (Accurately weighed *Nigella sativa* oil (100 mg) was transferred to a 10 ml volumetric flask and dissolved and diluted to the mark with 5% SLS solution to obtain a concentration of *Nigella sativa* oil equivalent to 10 mg/ml). The calibration curve was utilized to convert the absorbance value of the free oil into an equivalent amount.

So, the encapsulated oil amount was determined by the following formula:

$$\%\ \text{of encapsulated oil} = \frac{(amount\ of\ total\ oil - amount\ of\ free\ oil)}{(amount\ of\ total\ oil)} \times 100$$

### 2.4. Implementation of QbD Tools

QbD tools were employed to formulation development studies where QTPP and CQAs were created upon the clinical, pharmacokinetic (low bioavailability) and physicochemical features (strongly hydrophobic solubility) of NSO. A QTPP was well-defined (see Table **1**) to direct the development of chitosan nanocarrier and constructed on the QTPP,

the Critical Quality Attributes (CQAs) of the drug product has been recognized (represented in Table **2**).

Table **1** showed the QTPP for NSO-chitosan nanoparticles whilst Table **2** showed the Critical Quality Attributes (CQAs) of the drug product.

#### *2.4.1. Critical Material Attributes (CMAs)*

To develop proficient nanoparticles, it has been presumed that formulation polymeric nanoparticles rely upon numerous factors, such as particle size, types of solvents and polymers used in the synthesis, area of application, *etc*. As such to decide the critical material attributes, all formulation variables have been assessed with a deeper risk evaluation offered in Table **3**. Additional formulation development studies were conducted according to the recognized control strategy in Table **3**.

#### *2.4.2. Selecting Polymer Concentration and Cross Linker Types by One Factor at a Time (OFAT)*

Before the optimization study, polymer concentration selection and selection of the crosslinker had been performed by OFAT methodology. Based on the OFAT strategy, just 5 experimental runs were found to be enough for identifying the polymer concentration and cross linker type, for the statistical optimization study. For this purpose, various formulations have been prepared, and formulation behaviors mainly particle size were estimated.

### 2.5. Formulation Optimization Study with Full Factorial Design

Following selection of processing parameters by OFAT studies, a randomized statistical full factorial design was performed for two independent factors for the optimization of the chitosan nanoparticles formulation; the stirring rate (A) and chitosan to benzoic acid ratio (B). STATGRAPHICS® Centurion XVII Version software was used for statistical experimentation. Nine batches were prepared and evaluated for particle size (Y1), polydispersity index (Y2) and encapsulation efficacy (Y3). Mathematical equations were created for the prediction of all determined responses and a design interpretation was developed by contour plots and response surface graphics.

### 2.6. Physicochemical Characterization of CS-NPs

#### *2.6.1. Particle Size (PS) and Particle Distribution (PDI)*

Dynamic light scattering technique using Zetasizer Nano ZS. (Malvern, UK) was employed to verify the PS and PDI. Redispersion of the NPs(20µl) in 15 mL deionized water followed by 10 min sonication prior to estimation. All samples were estimated in triplicates and results were signified as mean value ± SD [18].

#### *2.6.2. Transmission Electron Microscopy*

Fabricated NPs morphology (plain or medicated) was resoluted by Transmission Electron Microscopy (TEM). Investigated samples were generated by suspending a small amount of NPs dispersion into deionized water (5 mL). A small amount of the developed sample was located on a paraffin pane and a grid coated with carbon was placed for 1 min to let CS-NPs stick to the carbon grid. Removal of the residual dispersion was done by adsorbing the rest with the corner of a filter paper. Samples were air dried before microscopic examination with no staining [20].

#### *2.6.3. Scanning Electron Microscopy (SEM) of Nanoparticles*

Samples were scattered on SEM pouch with two-fold sided sticky tape, covered with a coat of 150 Å gold for 2 min by means of a SPI module TM gold sputter coater and estimated utilizing the high vacuum approach [21, 22].

### 2.7. *In vitro* Release Studies

Dialysis technique was utilized to perform the *in vitro* release study of the optimized formula. Briefly, a Phosphate Buffered Saline (PBS) solution was used to soak and rinse the dialysis sac. NSO loaded nanoparticles resuspended in 3 mL of PBS solution were placed in the dialysis sac, hence, surrounded by 50 mL of PBS containing 5% SLS (To lessen aggregation and release oil consistently [2] at pH 7.4.

**Table 1. Quality Target Product Profile (QTPP) for chitosan nanoparticles.**

| QTPP Element | Target |
|---|---|
| Dosage form | Polymeric nanoparticles |
| Route of administration | Oral |
| Stability | Stable at least 6-month shelf life at long term stability conditions |
| Physical properties | Should have a particle size in nano range. |

**Table 2. Critical Quality Attributes (CQAs) of polymeric nanoparticles.**

| CQAs | Target | Justification of Criticality |
|---|---|---|
| Particle size | 100-500 nm | In nanorange to improve permeation and bioavailability |
| PDI | 0.1-0.3 | Low as much as possible to reveal the mono-dispersity of the synthetized nanoparticles. |
| Encapsulation efficacy | >80% | To get much more amount of drug encapsulated in nano range |

**Table 3. Risk assessment* of Critical Material Attributes (CMAs) on drug product CQAs, with control strategies.**

| Drug Product CQAs Assay | Formulation Variables | | | | |
|---|---|---|---|---|---|
| | Polymer Conc. | Cross Linker | Stirring Rate | Polymer to Cross Linker Ratio | Centrifugation Force |
| Particle size | Conc. should be identified and fixed by OFAT. | Type should be identified and fixed by OFAT. | Level Range should be identified and fixed within DoE Design. | Level Range should be identified and fixed within DoE Design. | Medium |
| PDI | Low | Low | Level Range should be identified and fixed within DoE Design. | Level Range should be identified and fixed within DoE Design. | Medium |
| Encapsulation efficacy | Low | Low | Level Range should be identified and fixed within DoE Design. | Level Range should be identified and fixed within DoE Design. | Low |

*** *Relative risk ranking***: Low risk: no further investigation is needed.; Medium risk: further investigation may be needed (by literature review).; High risk: the further investigation is needed.

Time-dependent release study (from 0 to 12h) was performed. The study was performed at 37°C with 50 rpm. At definite time intervals, 3 mL of the supernatant was removed, replaced with a fresh medium of PBS containing 5% SLS at pH 7.4 and measured spectrophotometrically.

### 2.8. Microbiological Assay

The microbiological activity of NSO CS-NPs dispersion was evaluated against test microorganism (*S. aureus*; ATCC® 25923). Seeded nutrient agar with the *S. aureus* was left to solidify in the petri dish. At a suitable distance, a definite amount (0.2 mg containing 0.196 mg of oil) of the dispersion and an equivalent amount of pure oil were carefully cupped into the agar layer [23]. The plates containing the seeded agar with the nanoparticles compared to pure oil were incubated at 37± 0.5°C for 24h. The zone of inhibition was measured subsequently to inoculation.

### 2.9. *In vitro* Cytotoxicity Study

The *in vitro* cytotoxicity of the encapsulated, as well as the NSO, was evaluated using the MTT assay. MTT (methyl thiazolyl-diphenyl-tetrazolium bromide) assay was conducted using two different cell lines (*i.e*. HCT 116 for colorectal carcinoma and PC3 for prostatic cancer). Results were expressed as a percentage of cell viability as compared to the control *versus* concentration. The concentration at which 50% of growth is inhibited (IC50) was determined using GraphPad prism 5.0 software (Graphpad Software, La Jolla, CA, USA). The obtained results were represented as means ± SD from at least three separate experiments. MTT assay was performed in the following manner: cells were first seeded in 96-well plates ($2\times10^3$ cells/well) and incubated for 24 h at 37°C in 5% $CO_2$ environment. At that point, the cells were treated with NSO injection and NSO-CN-NPs, respectively, leaving the untreated cells as a control, and the cells were cultured for 24h, 48h and 72h. Then, 20 µl of MTT solution (5 mg/ml) was added to each well and the culture was continued for 4h. The medium was then removed and 150 µl of DMSO was added per well and measured at 490 nm. The relative cell viability is estimated as follows:

$$\%\ \text{relative cell viability} = \frac{\text{test group OD}}{control\ group\ OD} \times 100\%$$

## 3. RESULTS AND DISCUSSION

### 3.1. Preparation of CS-NPs

BA and Ci were selected in this study since they are considered safer than other known linkers such as glutaraldehyde and glycol which are toxic and have lots of side effects such as eye, skin and respiratory tracts irritation, headache, vomiting, fatigue and asthma [24].

Moreover, AitBarka *et al*. [25] reported that CS not only decreases the growth of pathogens but apparently it causes morphologic and structural alterations in bacteria molecules.

In the present study, CS was used in formulating CS-Ci and CS-BA nanoparticles to take advantage of the above mentioned CS's features.

### 3.2. Implementation of QbD Tools

#### *3.2.1. Determination of Critical Material Attributes (CMAs)*

To regulate the critical material attributes, all formulation variables have been appraised with a deeper risk assessment presented in Table **3**. Further formulation development studies were conducted according to the identified control strategy in Table **3**.

**Table 4. OFAT formulations and determined values for the responses.**

| Batch No. | OFAT Group | Type | Fixed Parameters | Measured Response (P.S.) |
|---|---|---|---|---|
| B1 | Chitosan conc. Selection | 3% | 2% NSO | 2.3 μm |
| B2 | | 2% | Stirring rate 2000 | 1.8 μm |
| B3 | | 1% | Mixing time 30 min | 1.6 μm |
| B4 | Cross linker selection | Cinnamic acid | 2% NSO | 2.5 μm |
| B5 | | Benzoic acid | Stirring rate 2000 | 1.5 μm |
| | | | Mixing time 30 min | |

### *3.2.2. Selecting Polymer Concentration and Cross Linker Types by OFAT*

Table **4** showed the OFAT strategy where just 5 experimental runs were found to be enough for identification of polymer concentration and cross linker type, as a prerequisite step, for the statistical optimization study.

Three concentrations of chitosan/acetic acid solutions namely 1, 2 and 3% were investigated for particle size whereas the lower conc. of chitosan revealed smaller particle size also, the crosslinking by BA revealed smaller particle size than Ci may be explained by greater molecular weight in case of Ci.

CS concentration is possibly the most important determinant of the physicochemical characteristics of the CS-NPs. Table **3** showed the effect of CS concentrations on the particle size of CS-NPs. The particle size was linearly increased from 1.6±0.32 to 2.3±0.25 μm by increasing CS concentration from 1 to 3 mg/ml [26]. These results were also in agreement with previously published reports [27-30].

The increase in particle size was expected to be due to the presence of inter-molecular hydrogen bonding (due to-OH groups) and inter-molecular electrostatic repulsion (due to-$NH3^{+}$groups) which exist along the outline of CS [31].

As the CS concentration increases, a single larger particle is formed as more CS molecules tend to entangle with each other and crosslink with counter ion (BA) [30].

Larger particles (with high values as 2.3±0.25 μm) were obtained when the chitosan content in the matrix was increased. Moreover, narrower size distribution was obtained as the chitosan proportion is increased which was also observed for chitosan-polyglutamic acidic matrixes in the study [32].

The most likely explanation is that increasing the chitosan proportion in matrix reduces the gum-chitosan interactions and consequently supports the formation of particles bonded by hydrogen chitosan interactions between their chains (interchain interactions). The positive amino group of chitosan causes repulsion between the chains, leading to high nanoparticle sizes [32].

Regarding the choice of crosslinked fatty acid, the obtained results were in accordance with Beyki *et al*. [33] and revealed that bigger PS is obtained with cinnamic acid. As the cinnamic acid is a large "bulkier" polymer than benzoic acid leading to a high degree of entanglement and less efficient packing of the polymer chains, resulting in less expulsion of water from the inner structure. Effect of the concentration and molecular weight on the size of nanoparticles prepared has been previously described for chitosan–TPP nanoparticles and various other nanoparticles compositions [27, 34, 35].

Considering the abovementioned features of CS and BA, in the present study, CS-BA nanoparticles were synthesized by self-assembly method that led to the formation of non-polar heads inside-ward and polar heads outside-ward.

The BA and CS concentrations and ratios were determined so that 75 carboxyl groups of BA were available for each 100 amine groups of CS [36, 37]. This ratio not only led to the formation of homogeneous nanoparticles (monodisperse) with spherical morphology but also the extra available amine groups (not bound) caused the produced nanoparticles to be hydrophilic.

The monodispersity of the synthesized nanoparticles was revealed by the obtained microscopic images and the size distribution of the synthesized nanoparticles particles (see Fig. **1**).

### *3.2.3. Particle Size and Size Distribution (PS and PDI) of NSO Nanoparticles*

A particle size ranged from 361-1750 nm (Fig. **1a**) with a dispersant RI 1.4 with a viscosity (cP) equals 0.88 was considered optimum for nanoparticle formulation.

### *3.2.4. Electron Microscopy*

SEM and TEM micrographs showed the globular (spherical) structure of the self-assembled nanoparticles with the particle size of less than 300 nm (Fig. **1b** and **c**). The monodispersity of the synthesized nanoparticles was revealed by the microscopic images. Fig. (**1a**) revealed the size distribution of the synthesized nanoparticles [36]. The morphology of the selected formula of NSO-loaded chitosan nanoparticles was investigated. Vesicles diameter of < 200 μm revealed the presence of well identified spherical nanoparticles existing in disperse pattern.

In this study, the size of the developed nanoparticles was considered satisfactorily small which was attributed to numerous intended manufacturing procedures; first, the initial sonication performed converted the long chains of CS to smaller pieces and prevented the formation of long-chained nanoparticles. Other factors that could have contributed to lowering particles size were the re-sonication and the passage of the nanoparticles through the filter.

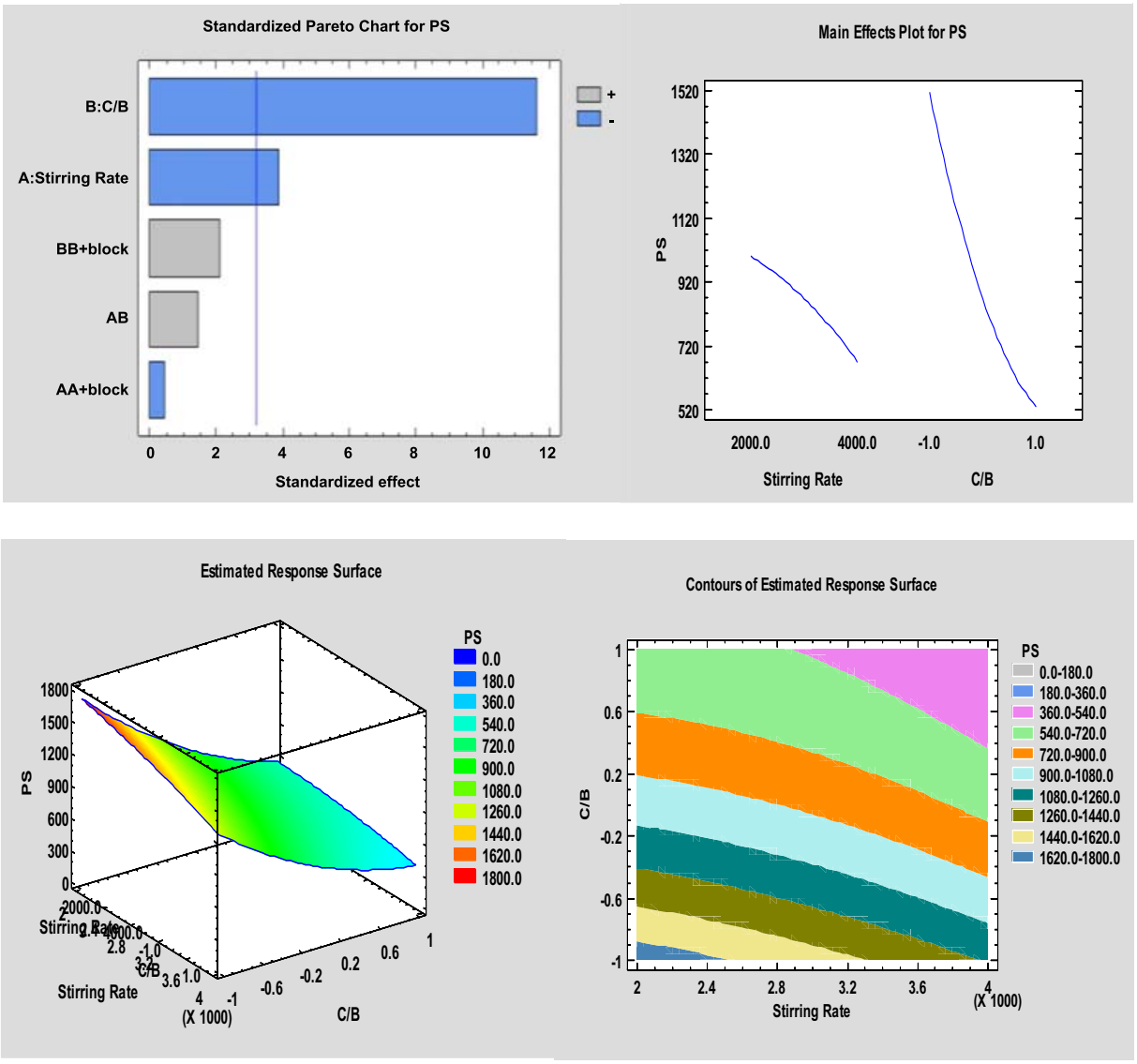


**Fig. (1a).** Factors affecting particle size (**A**). Pareto chart, (**B**). Main effects chart, (**C**). Response Surface, and (**D**). Contour plot. (*A higher resolution / colour version of this figure is available in the electronic copy of the article*).

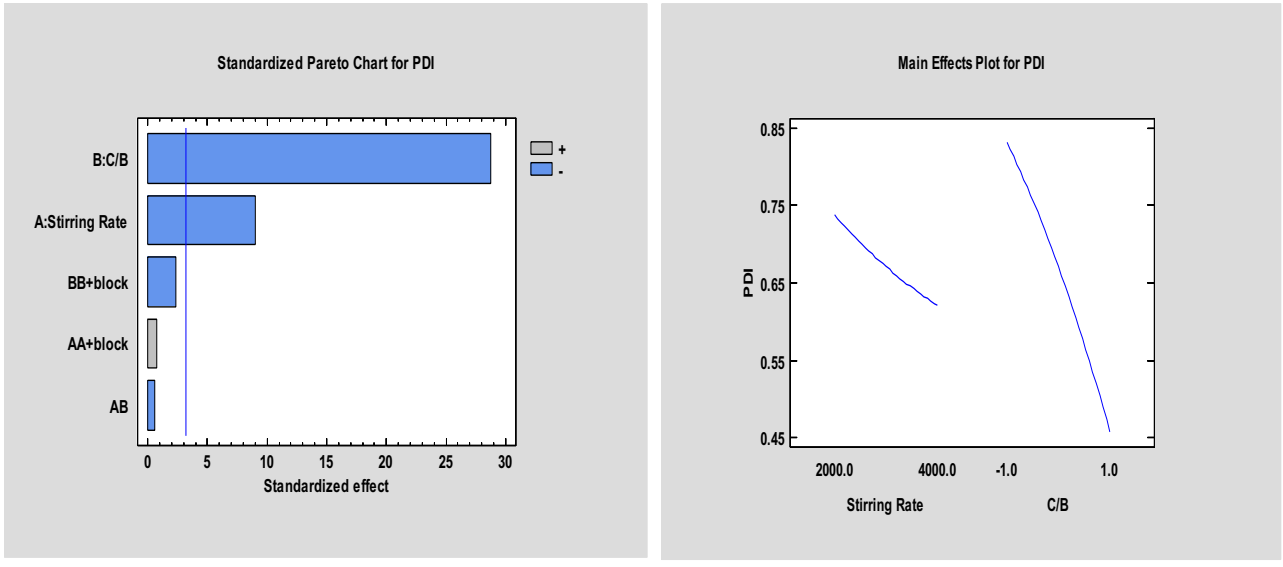


**Fig (1b) contd…**

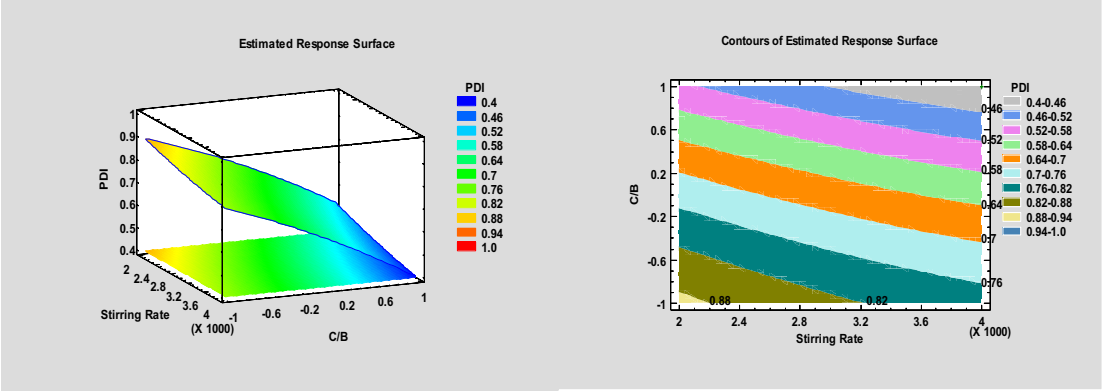


**Fig. (1b).** Factors affecting PDI (**A**). Pareto chart, (**B**). Main effects chart, (**C**). ResponseSurface, and (**D**). Contour plot. (*A higher resolution / colour version of this figure is available in the electronic copy of the article*).

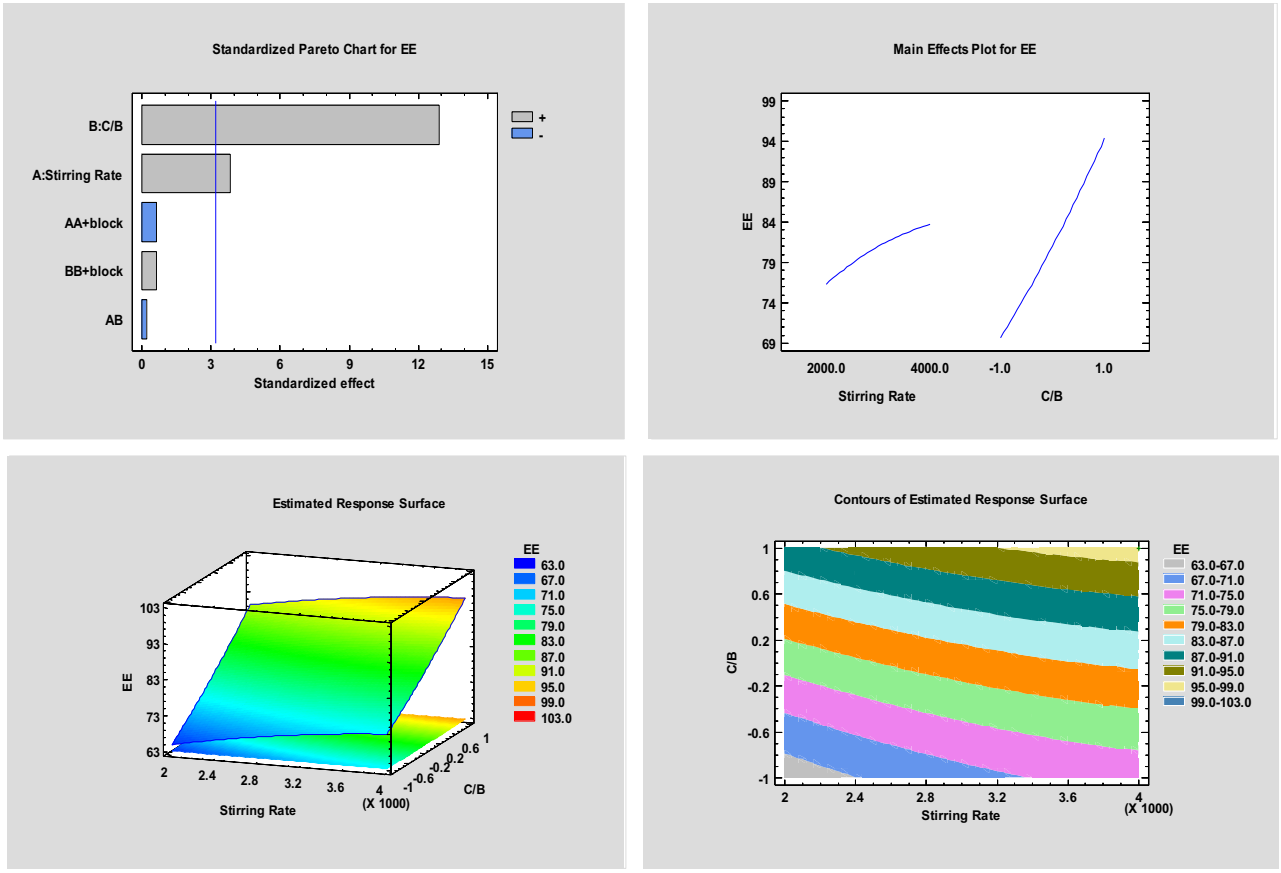


**Fig. (1c).** Factors affecting E.E. (**A**). Pareto chart, (**B**). Main effects chart, (**C**). ResponseSurface, and (**D**). Contour plot. (*A higher resolution / colour version of this figure is available in the electronic copy of the article*).

### 3.3. General Full Factorial Design (Two Factors with Three Levels as Numeric Variables)

Design of experiment (DoE) using (Statgraphics XVII) ® program was implemented where all factors affecting the three investigated responses were varied together. Preliminary investigations by using QbD tools were used to select the initial variables with the appropriate levels.

#### *3.3.1. Factorial Experimental Design*

Optimization of the NSO encapsulated nanoparticles was conducted using randomized general full factorial ($2^3$) experimental design. Factors, responses, and targets are presented in Table **5**. The design investigated the effect of two independent variables at three different levels (-1, 0, and + 1, demonstrating low, medium, and high, respectively) giving up nine experimental runs (assigned F1–F9) (Table **6**).

The selected factors were the stirring rate (X1, a crucial factor in first emulsification) and CS/BA ratio (X2, the main backbone of nanoparticles) while the variable responses investigated were (1) particle size (Y1), (2) PDI (Y2), (3) Encapsulation Efficacy (Y3). Other formulation compositions and processing method were held constant.

The studied factors included: (A: Stirring Rate) beginning with 2000 rpm as the lowest level (-1), 4000 rpm as the highest level (+1) and 3000 rpm as center point (0). (B:

**Table 5. Factors, levels, responses and targets for the full factorial design.**

| Factors | | Levels | | |
|---|---|---|---|---|
| | | **-1** | **0** | **+1** |
| A | Stirring rate | 2000 | 3000 | 4000 |
| B | Chitosan/ Benzoic acid ratio | 1:2 | 1:1 | 2:1 |
| Responses | | Target | | |
| Y1 | Particle size | Minimize | | |
| Y2 | Polydispersity index | Minimize | | |
| Y3 | Encapsulation efficacy | Maximize | | |

**Table 6. General full factorial design of experiment by (StatgraphicsXVII)® program.**

| Formulae | Independent Variables | | Responses | | |
|---|---|---|---|---|---|
| Run | Stirring Rate | C/B | PS | PdI | EE |
| | Rpm | Ratio | nm | | % |
| 1 | 4000.0 (+1) | 1:1 (0) | 780 | 0.63 | 83 |
| 2 | 4000.0 (+1) | 1:2 (-1) | 1200 | 0.78 | 72 |
| 3 | 2000.0 (-1) | 1:1 (0) | 910 | 0.72 | 78 |
| 4 | 4000.0 (+1) | 2:1 (+1) | 341 | 0.4 | 98 |
| 5 | 2000.0 (-1) | 1:2 (-1) | 1780 | 0.901 | 63 |
| 6 | 2000.0 (-1) | 2:1 (+1) | 620 | 0.54 | 90 |
| 7 | 3000.0 (0) | 1:1 (0) | 850 | 0.68 | 80 |
| 8 | 3000.0 (0) | 1:2 (-1) | 1500 | 0.83 | 72 |
| 9 | 3000.0 (0) | 2:1 (+1) | 562 | 0.45 | 93 |

CS/BA ratio, with 1:2 as the low level (-1), 2:1 as the high level (+1) and 1:1 as center point (0)). The design selected was 3-level factorial design: 3^2 with quadratic response

Statgraphics XVII® program created graphs showing the effect of the two significant variables as a surface in three-dimensional space (Fig. **2**) and by interpreting the developed contour plots and surface plots, the following assumptions could be drawn: the stirring rate (variable A) was optimum at the highest level (+1) meaning that smaller particle size could be obtained by increasing the stirring rate which was in accordance with Zhu *et al.* [38]. Chitosan/benzoic acid molar ratio (variable B) showed the lowest Particle size and the highest encapsulation efficacy at the same level (*i.e*. the highest level (+1); *see* Figs. (**2a** and **2c**) segments A & C).StatgraphicsXVII® program created a linear equation between each investigated variable and the independent levels (Stirring Rate and C/B ratio). The developed equations were created by conducting the analysis of variance and were represented in Table **7**. Statistically, *p*-value less than 0.05 was considered "statistically significant" for any factor studied. From statistical point of view, a significant relationship between the variables at the 95.0% confidence level is crystal clear since the *p*-values in the ANOVA analysis (in Table **7**) for the three investigated responses were less than 0.05.

### 3.4. Optimization of CS: BA Molar Ratio

One of the prime parameters to control the particle size and size distribution is CS: BA molar ratio. Therefore, a wide range of Cs: BA molar ratios (2:1 to 1:2) were assessed with constant CS concentration (1%) .The highest particle size was obtained with the lowest CS: BA molar ratio (1:2) and the particle size decreased linearly by increasing CS: BA molar ratio to 2:1 (see Fig. **2a** segment **B**). These results were in agreement with previously published data [28]. Hu and co-workers reported that the higher BA concentration, the more turbid the suspension became, indicating the formation of particle agglomerates when superfluous BA connects individual nanoparticles. The reduction in the NPs zeta potential that took place as the CS: BA molar ratios increased leading to electrostatic interaction (promoting aggregate formation) between the NPs might be the proper cause for the observed increment in the particle size [39].

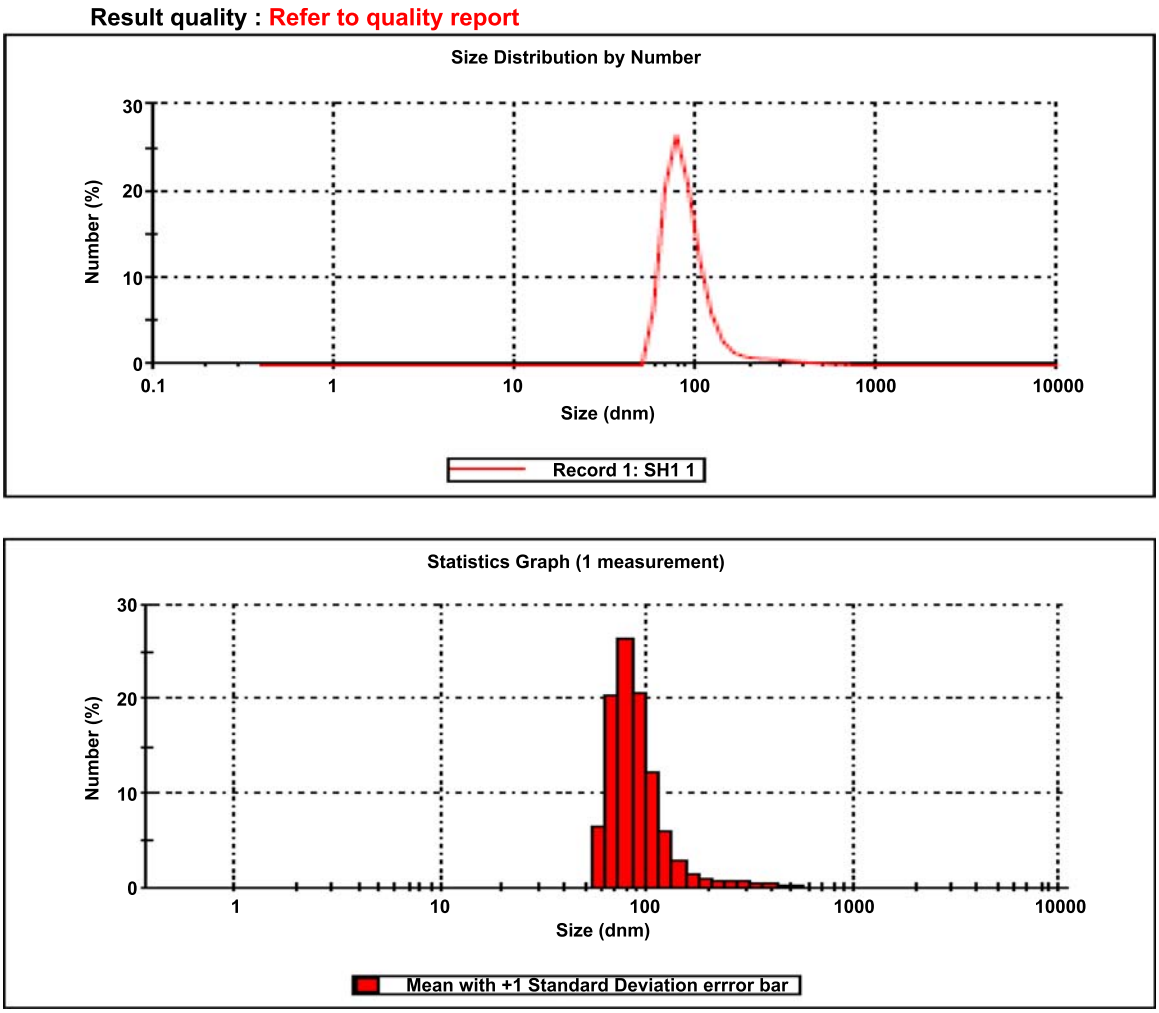


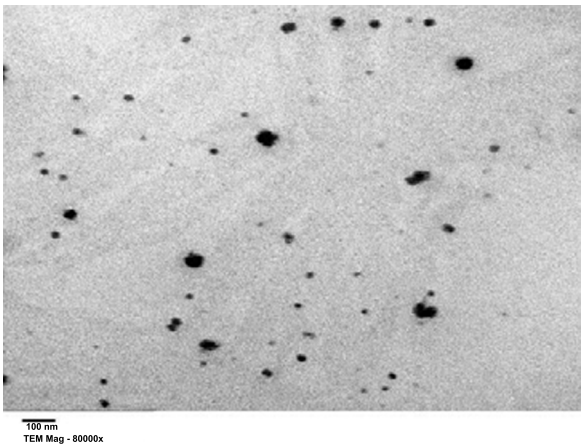


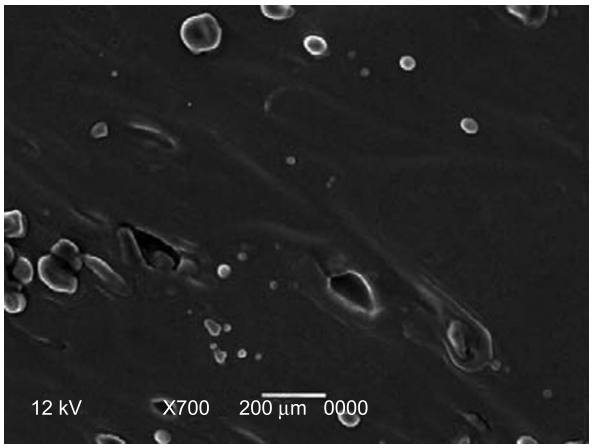


**Fig. (2).** particle size and particle size distribution (**a**) Transmission electronmicroscopy (**b**) and Scanning Electron Microscope (**c**) of formed NSO nanoparticles. (*A higher resolution / colour version of this figure is available in the electronic copy of the article*).

### 3.5. Optimizations of Stirring Speed

The results obviously showed that the stirring rate had a significant impact on the particle size and polydispersity index of the resulting NPs as shown in (Fig. **2**). By increasing the stirring speed from 2000 rpm to 4000 rpm, the mean particle size reduced gradually from 1780±35 nm to 341±62 nm (Fig. **2**). These results were also in agreement with the previously published study [34] which reported the significant impact of stirring speed on the particle size and size distribution of nano-carriers. Fan and co-workers [30] also reported that increasing the stirring speed from 200 rpm to 800 rpm led to significant narrowing the particle size distribution. Their findings led to the suggestion that the

**Table 7. Analysis of variance.**

| Source | Sum of Squares | Df | Mean Square | F-Ratio | P-Value |
|---|---|---|---|---|---|
| Particle Size | | | | | |
| Model | 1.62033E6 | 2 | 810164. | 46.57 | 0.0002 |
| Residual | 104391. | 6 | 17398.5 | | |
| Total (Corr.) | 1.72472E6 | 8 | - | | |
| Equation | | | PS = 1443.72 - 0.164833*Stirring Rate - 492.833*C/B | | |
| PDI | | | | | |
| Model | 0.229974 | 2 | 0.114987 | 287.67 | 0.0000 |
| Residual | 0.0023983 | 6 | 0.000399722 | | |
| Total (Corr.) | 0.232372 | 8 | - | | |
| Equation | | | PDI = 0.8345 - 0.0000585*Stirring Rate - 0.186833*C/B | | |
| EE | | | | | |
| Model | 993.333 | 2 | 496.667 | 144.19 | 0.0000 |
| Residual | 20.6667 | 6 | 3.44444 | | |
| Total (Corr.) | 1014.0 | 8 | - | | |
| Equation | | | EE = 70.0 + 0.00366667*Stirring Rate + 12.3333*C/B | | |

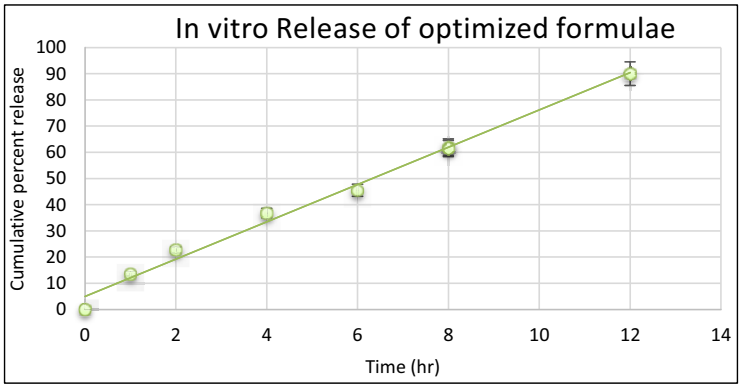


**Fig. (3).** *In vitro* release of optimized NSO chitosan nanoparticles formulae. (*A higher resolution / colour version of this figure is available in the electronic copy of the article*).

dispersion of BA in chitosan solution could be accelerated by adequate stirring and the increased shear force helps to narrow dispersity index; however, intense stirring may destroy the repulsive force between particles causing particles aggregation. By comparing the low to the high stirring speeds, it was concluded that the moderate stirring rate improves the mixing and creates a more uniform environment for NPs formation, therefore the resulting particles exhibit narrow dispersity observed through PDI analysis which highlights a gradual decrease in the dispersity range of CS-BA-NPs from 0.9±0.04 to 0.4±0.02, when the stirring speed was increased from 2000 rpm to 4000 rpm.

### 3.6. Optimization of Centrifugation Conditions

Centrifugation is one of the integral process parameter affecting the particle size, PDI and percent actual yield of the NPs [26]. At the centrifugation speed (15000 rpm), the NPs isolated in the supernatant and sediment had shown approximately similar mean particle size.

### 3.7. *In vitro* Release Study

The release of the essential oil-loaded CS-BA nanoparticles at pH 7.4 was represented in Fig. (**3**) and it was obvious that approximately 90% of the encapsulated NSO was released over a time period of 12 hr representing the release pattern in the bloodstream. Therefore, more oil will be absorbed into the blood system and transported *via* the blood circulatory system to the infection site more efficiently than free oil (*i.e*. oil is not encapsulated in the nanoparticles).

### 3.8. Microbiological Studies

Clear inhibition zones were obtained in optimized formulation against test organisms namely *S. aureus* represented in

Fig. (**4**). Formulating NSO in nanoparticles showed uniform, even clear inhibition zone and much bigger (diameter of inhibition zone = 5.5 cm) than bare oil (diameter of inhibition zone = 3.6 cm) which is in accordance with a study conducted by Zivanovic and Chi [40], higher antimicrobial activity was gained in case of CS films enriched with various essential oils than CS films and free essential oils during a 5-day period.

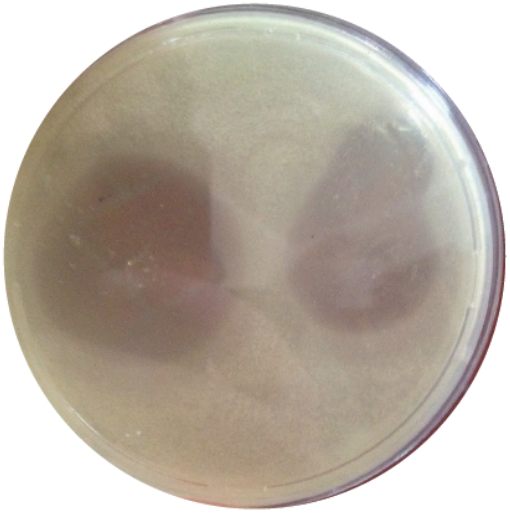

**Fig. (4).** Microbiological assay of NSO chitosan nanoparticles. (*A higher resolution / colour version of this figure is available in the electronic copy of the article*).

### 3.9. *In vitro* Cytotoxicity Study

The *in vitro* cytotoxicity of the optimized encapsulated oil formula against two different cell lines (*i.e*. HCT 116 for colorectal carcinoma and PC3 for prostatic cancer) was evaluated using MTT assay. Fig. (**5**) represented the results of the conducted *in vitro* cytotoxicity study. MTT gets reduced to purple formazan by mitochondrial reductase in living cells. This reduction takes place in the presence of active reductase enzymes, and hence, this conversion is used as a measure of viable (living) cells [41, 42]. The conducted *in vitro* cytotoxicity revealed that either for free oil or encapsulated oil, there was a concentration-dependent cell viability and the encapsulated oil showed a high level of cell viability inhibition.

The IC50 of the optimized encapsulated oil formula (17.95 ±0.82 µM) was found to be 2.5 fold less than the free oil (43.56 ±1.95 µM) after 48 h of incubation in case of HCT 116 cell line and the IC50 of the optimized encapsulated oil formula (4.02 ±0.12 µM) was found to be 7 fold less than the free oil (29.72 ±1.41 µM) after 48h of incubation in case of PC3cell line as can be deducted from (Fig. **5**). The existence of different powerful anticancer components particularly thymoquinone might be responsible for the decrease in cancer cell viability. The best explanation for this behavior is the ability of the encapsulated oil to deliver the oil to individual cells, unlike the free oil which fails to reach the cells individually owing to its hydrophobicity. The observed toxicity behavior is totally attributed to the encapsulated oil since the nontoxic nature of the nanocarrier was confirmed by the high percentage of the viability of treated cells (98%). Increasing the amount of NSO is expected to have greater toxic activity and the developed nanocarrier is well suited for these kinds of drug-delivery applications. These data was declared by many patents as in the study [43-47].

## CONCLUSION

CS-BA nanoparticles were formulated using ionic gelation method and QbD tools were used to identify the optimum factors for optimization. The optimized formula formulated by chitosan to benzoic acid ratio (2:1) with stirring rate (4000 rpm) had minimum-sized particles and the highest EE (*i.e*. 341 nm and 98%). Screening of the microbiological activity conducted against *S. aureus* showed bigger and uniform inhibition zone than the bare oil (inhibition zone diameter was 5.5 cm for encapsulated oil *vs* 3.6 cm for bare oil). The *in vitro* cytotoxicity showed that the nanoparticulated oil is more efficient than the free oil in suppressing the cancer cell viability (indicated by the lower IC50 obtained for the encapsulated oil).

## CURRENT & FUTURE DEVELOPMENTS

The current study utilized *in vitro* methods to investigate the potentials of encapsulated *Nigella sativa* oil. The future

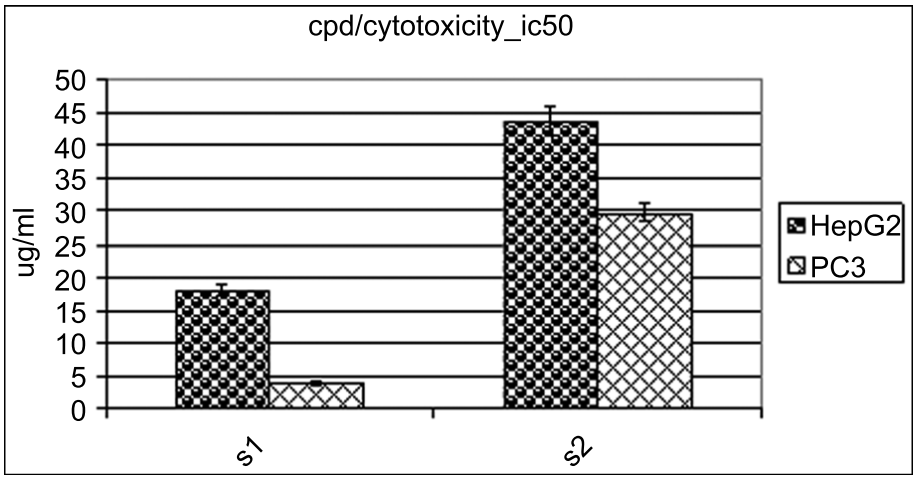


**Fig. (5).** IC50 of NSO chitosan nanoparticles: s1(nano formulated NSO) vs s2 (free oil). (*A higher resolution / colour version of this figure is available in the electronic copy of the article*).

completion of this work will aim to conduct *in vivo* animal studies. Poor biopharmaceutical properties and stability issues had hindered the clinical benefits of nigella sativa. Nanoparticulate drug delivery systems could be one of the useful techniques in bringing forth this miraculous oil into clinical reality.

## ETHICS APPROVAL AND CONSENT TO PARTICIPATE

Not applicable.

## HUMAN AND ANIMAL RIGHTS

No Animals/Humans were used for studies that are base of this research.

## CONSENT FOR PUBLICATION

Not applicable.

## AVAILABILITY OF DATA AND MATERIALS

Not applicable.

## FUNDING

None.

## CONFLICT OF INTEREST

The authors declare no conflict of interest, financial or otherwise.

## ACKNOWLEDGEMENTS

The authors would like to thank Dr. Esam Rashwan, Head of the confirmatory diagnostic unit, VACSERA-EGYPT for conducting the *in vitro* cytotoxicity study.

## REFERENCES

[1] Mastrobattista E. Advanced drug delivery in motion. Int J Pharm 2013; 454(1): 517-20. https://doi.org/10.1016/j.ijpharm.2013.05.002

[2] Natrajan D, Srinivasan S, Sundar K, Ravindran A. Formulation of essential oil-loaded chitosan–alginate nanocapsules. J Food Drug Anal 2015; 23(3): 560-8. https://doi.org/10.1016/j.jfda.2015.01.001

[3] Sarmento B, Ribeiro A, Veiga F, Sampaio P, Neufeld R, Ferreira D. Alginate/chitosan nanoparticles are effective for oral insulin delivery. Pharm Res 2007; 24(12): 2198-206. https://doi.org/10.1007/s11095-007-9367-4

[4] Li S, Yunna C, Yali Z, *et al*. Preparation of 5-fluorouracil-loaded chitosan nanoparticles and study of the sustained release *in vitro* and *in vivo*. Asian J Pharm Sci 2017; 12: 418-23. https://doi.org/10.1016/j.ajps.2017.04.002

[5] Saydam M, Takka S. Development and *in-vitro* evaluation of pH-independent release matrix tablet of weakly acidic drug valsartan using quality by design (QbD) Tools, Drug Dev Ind Pharm 2018; 44(12): 1905-17. https://doi.org/10.1080/03639045.2018.1496450

[6] Duschatzky CB, Possetto ML, Talarico LB. Evaluation of chemical and antiviral properties of essential oils from South American plants. Antiviral Chem Chemother 2005; 16(4): 247-51. https://doi.org/10.1177/095632020501600404

[7] Akhtar MS, Degaga B, Azam T. Antimicrobial activity of essential oils extracted from medicinal plants against the pathogenic microorganisms: A review. Issue Biol Sci Pharm Res 2014; 2(1): 1-7.

[8] Al-Mariri A, Safi M. *In vitro* antibacterial activity of several plant extracts and oils against some gram-negative bacteria. Iran J Med Sci 2014; 39(1): 36-43. PMCid:PMC3895893

[9] Mukhtar H, Qureshi AS, Anwar F, Mumtaz MW, Marcu M. *Nigella sativa* L. seed and seed oil: Potential sources of high-valuecomponents for development of functional foods and nutraceuticals/pharmaceutical. J Essent Oil Res 2019; 31(3): 171-83. DOI:10.1080/10412905.2018.1562388. https://doi.org/10.1080/10412905.2018.1562388

[10] Sari Y, Dhadhang WK, Saryono N, Arington IG. Formulation and evaluation of nigella *Sativa oil* gel for accelerating diabetic wound healing. Asian J pharmabiolo Res 2014; 4: 16-22.

[11] Ahmad A, Hussain A, Mujeeb M, *et al*. Review on therapeutic potential of *Nigella sativa*: A miracle herb. Asian Pac J Trop Biomed 2013; 3: 337-52.

[12] Koroch AR, Rodolfo JH, Zygadlo JA. Bioactivity of essential oils and their components. In: berger r.g. (EDS) flavors and fragrances. Springer, Berlin, Heidelberg, Germany, 2007, pp. 87-115. https://doi.org/10.1007/978-3-540-49339-6_5

[13] Khan MA, Chen HC, Tania M, Zhang DZ. Anti-cancer activities of *Nigella sativa* (black cumin). Afr J Tradit Complem Alternat Med 2011; 8(5): 226-32. https://doi.org/10.4314/ajtcam.v8i5S.10.

[14] Nazzaro F, Coppola R, Fratianni F, De Martino L, De Feo D. Effect of essential oils on pathogenic bacteria. Pharmaceuticals 2013; 6(12): 1451-74. https://doi.org/10.3390/ph6121451

[15] Calvo P, Remunan-Lopez C, Vila-Jato JL, Alonso MJ. Chitosan and chitosan/ethylene oxide-propylene oxide block copolymer nanoparticles as novel carriers for proteins and vaccines. Pharm Res 1997; 14(10): 1431-6. https://doi.org/10.1023/A:1012128907225

[16] Vila A, Sanchez A, Tobio M, Calvo P, Alonso MJ. Design of biodegradable particles for protein delivery. J Control Release 2002; 78(1-3): 15-24. https://doi.org/10.1016/S0168-3659(01)00486-2

[17] Aktas Y, Andrieux K, Alonso MJ, *et al*. Preparation and *in vitro* evaluation of chitosan nanoparticles containing a caspase inhibitor. Int J Pharm 2005; 298(2): 378-83. https://doi.org/10.1016/j.ijpharm.2005.03.027

[18] Elnaggar YSR, Etman SM, Abdelmonsif DA, Abdallah OY. Intranasal piperine-loaded chitosan nanoparticles as brain-targeted therapy in alzheimer's disease: Optimization, biological efficacy and potential toxicity. J Pharm Sci 2015; 104(10): 3544-56. https://doi.org/10.1002/jps.24557.

[19] Snehalatha B, Momin M, Mishal AV, Kale TR. Development and validation of spectrophotometric method for simultaneous estimation of *Nigella sativa* seed oil and ginger extract in the same dosage form. Int J Pharm Sci Res 2014; 5(12): 1000-5. DOI:10.13040/IJPSR.0975-8232.5 (12).1000-05.

[20] Fazil S, Haque S, Kumar M, Baboota S, Sahni JK, Ali J. Development and evaluation of rivastigmine loaded chitosan nanoparticles for brain targeting. Eur J Pharm Sci 2012; 47(1): 6-15. https://doi.org/10.1016/j.ejps.2012.04.013

[21] Abd-Elbary A, El-laithy HM, Tadros MI. Sucrose stearate-based proniosomes derived niosomes for the nebulisable delivery of cromolyn sodium. Int J Pharm 2008; 357: 189-98. https://doi.org/10.1016/j.ijpharm.2008.01.056

[22] Arafa MG, Ayoub BM. DOE optimization of nano-based carrier of pregabalin as hydrogel: New therapeutic & chemometric approaches for controlled drug delivery systems. Sci Rep 2017; 7: 41503. https://doi.org/10.1038/srep41503.

[23] Sarath CC, Shirwalkar A, Kiron SS. Development and evaluation of chitosan containing ciprofloxacin β- CD complex. Int J Pharm Tech Res 2010; 2(1): 246-52.

[24] Natella F, Nardini M, Felice MD, Scaccini C. Benzoic and cinnamic acid derivatives as antioxidants: Structure-activity relation. J Agric Food Chem 1999; 47(4): 1453-9. https://doi.org/10.1021/jf980737w.

[25] Ait BE, Eullaffroy P, Clément C, Vernet G. Chitosan improves development, and protects *Vitis vinifera L.* against *Botrytis cinerea*. Plant Cell Reports 2004; 22: 608-14. https://doi.org/10.1007/s00299-003-0733-3 PMID: 14595516.

[26] Hussain Z, Sahudin S. Preparation, characterization and colloidal stability of chitosan-tripolyphosphate nanoparticles: Optimization of formulation and process parameters. Int J Pharm Pharm Sci 2016; 8(3): 297-308.

[27] Gan Q, Wang T, Cochrane C, McCarron P. Modulation of surface charge, particle size and morphological properties of chitosan-TPP nanoparticles intended for gene delivery. Colloids Surf Biointerfaces 2005; 44: 65-73. https://doi.org/10.1016/j.colsurfb.2005.06.001

[28] Hu B, Pan C, Sun Y, *et al*. Optimization of fabrication parameters to produce chitosan- tripolyphosphate nanoparticles for delivery of tea catechins. J Agric Food Chem 2008; 56: 7451-8. https://doi.org/10.1021/jf801111c

[29] Liu H, Gao C. Preparation and properties of ionically cross-linked chitosan nanoparticles. Polym Adv Technol 2009; 20: 613-9. https://doi.org/10.1002/pat.1306

[30] Fan W, Yan W, Xu Z, Ni H. Formation mechanism of monodisperse, low molecular weight chitosan nanoparticles by ionic gelation technique. Colloids Surf B 2012; 90: 21-7. https://doi.org/10.1016/j.colsurfb.2011.09.042

[31] Qun G, Ajun W. Effects of molecular weight, degree of acetylation and ionic strength on surface tension of chitosan in dilute solution. Carbohydr Polym 2006; 64: 29-36. https://doi.org/10.1016/j.carbpol.2005.10.026

[32] Hajdu I, Bodnár M, Filipcsei G, *et al*. Nanoparticles prepared by self-assembly of chitosan and poly-glutamic acid. Colloid Polym Sci 2008; 286: 343-50. https://doi.org/10.1007/s00396-007-1785-7.

[33] Beyki M, Zhaveh S, Khalili ST, *et al*. Encapsulation of menthapiperita essential oils in chitosan- Cinnamic acid nanogel with enhanced antimicrobial activity against *Aspergillus flavus*. Ind Crops Products. 2014; 54: 310-19. https://doi.org/10.1016/j.indcrop.2014.01.033

[34] Lapitsky Y. Ionically crosslinked polyelectrolyte nanocarriers: Recent advances and open problems. Curr Opin Colloid Interface Sci 2014; 19: 122-130. https://doi.org/10.1016/j.cocis.2014.03.014

[35] Paromita I, Jorrit JW, Adam B, Jukka R. Chitosan-based nanoembedded microparticles: Impact of Nanogel composition on physicochemical properties. Pharmaceutics 2017; 9: 1. https://doi.org/10.3390/pharmaceutics9010001 PMCid:PMC5374367

[36] Khalili ST, Mohsenifar A, Beyki M, *et al*. Encapsulation of thyme essential oils in chitosan-benzoic acid nanogel with enhanced antimicrobial activity against *Aspergillus flavus*. LWT-Food Sci Technol 2015; 60: 502-8. https://doi.org/10.1016/j.lwt.2014.07.054

[37] Chouhan S, Sharma K, Guleria S. Antimicrobial activity of some essential oils- Present status and future perspectives. Medicines 2017; 4: 58. https://doi.org/10.3390/medicines4030058.

[38] Zhu HJ, Liu XM, Yangn H, Shen XD. Effect of the stirring rate on physical and electrochemical properties of LiMnPO4 nanoplates prepared in a polyol process. Ceram Interfaces 2014; 40: 6699-704. https://doi.org/10.1016/j.ceramint.2013.11.131

[39] Papadimitriou S, Bikiaris D, Avgoustakis K, Karavas E, Georgarakis M. Chitosan nanoparticles loaded with dorzolamide and pramipexole. CarbohydrPolym 2008; 73: 44-54. https://doi.org/10.1016/j.carbpol.2007.11.007

[40] Zivanovic S, Chi SD. Antimicrobial activity of chitosan films enriched with essential oils. J Food Sci 2005; 70: 45-51. https://doi.org/10.1111/j.1365-2621.2005.tb09045.x

[41] Mulik RS, MOnkkOnen J, Juvonen RO, Mahadik KR, Paradkar AR. ApoE3 mediated polymeric nanoparticles containing curcumin: Apoptosis induced *in vitro* anticancer activity against neuroblastoma cells. Int J Pharm 2012; 437: 29-41. DOI:10.1016/j.ijpharm.2012.07.062

[42] Saxena V, Hussain MD. Polymeric mixed micelles for delivery of curcumin to multidrug resistant ovarian cancer. J Biomed Nanotechnol 2013; 9(7): 1146-54. DOI: 10.1166/jbn.2013.1632.

[43] Crooks, P.A., Worthen, D.R., Ghosheh, O.A. Use of naturally occurring Quinones TQ and Di-TQ as anti-neoplastic and cytotoxic agent. US006218434B1 (**1999**).

[44] Mazzi, E.A., Soliman, K.F. Nutraceutical composition and method of use for the treatment of cancer. US201002093889 (**2010**).

[45] Sarkar, F.H., Mohammad, R.M.T.Q. Analogue for treatment of pancreatic cancer. US2011126544 (**2011**).

[46] Odeh, F., Ismail, S. Liposomal formulations comprising Thymoquinone and Taxane, and method of treating cancer using same. WO2016005786A1 (**2016**).

[47] Salem, A.E., Ismail-El, H., Ibrahim, A., Abdu, A., Samir, A. Thymoquinone derivatives for the treatment of cancer. WO2016024145A1 (**2016**).